The E3 ubiquitin ligase MARCH3 controls the endothelial barrier

Héloïse M Leclair, Gwennan André-Grégoire, Lucas Treps, Sandy Azzi, Nicolas Bidère, Julie Gavard

The E3 ubiquitin ligase MARCH3 controls the endothelial barrier

Héloïse Leclair, Gwennan André-Grégoire, Lucas Treps, Sandy Azzi, Nicolas Bidère, Julie Gavard

Received Date : 22-Jun-2016
Revised Date : 01-Sep-2016
Accepted Date : 06-Sep-2016
Article type : Research Letter

THE E3 UBIQUITIN LIGASE MARCH3 CONTROLS THE ENDOTHELIAL BARRIER

Héloïse M Leclair[a,b,c], Gwennan André-Grégoire[a,b], Lucas Treps[c], Sandy Azzi[c], Nicolas Bidère[a,b,c], Julie Gavard[a,b,c*]

a CRCINA, CNRS, INSERM, Université de Nantes, 8 quai Moncousu, F-44007, Nantes, France
b Team SOAP, "Signaling in Oncogenesis, Angiogenesis, and Permeability", 8 quai Moncousu, F-44007, Nantes, France
c Institut Cochin, CNRS, INSERM, Université Paris Descartes, 22 rue Méchain, F-75014, Paris, France

* Correspondence to: Julie Gavard, CRCNA, SOAP team, Room 416, 8 quai Moncousu, ntes 44007, France
Email: julie.gavard@inserm.fr, Phone: +33 2 2808 0327, Twitter: @LabSoap

Running head: MARCH3 function in endothelial cells

Keywords: occludin, claudin-5, tight junction, permeability, ubiquitin, FoxO

Abstract

Cell-cell contacts coordinate the endothelial barrier function in response to external cues. To identify new mediators involved in cytokine-promoted endothelial permeability, we screened a siRNA library targeting E3 ubiquitin ligases. Here, we report that silencing of the late endosome/lysosomal membrane-associated RING-CH-3

(MARCH3 enzyme protects the endothelial barrier. Furthermore, transcriptome analysis unmasked the upregulation of the tight junction-encoding gene occludin (*OCLN* in MARCH3-depleted cells. Indeed, MARCH3 silencing results in the strengthening of cell-cell contacts, as evidenced by the accumulation of junctional proteins. From a molecular standpoint, the FoxO1 forkhead transcription repressor was inactivated in the absence of MARCH3. This provides a possible molecular link between MARCH3 and the signaling pathway involved in regulating the expression of junctional proteins and barrier integrity.

Introduction

The vascular endothelium forms a semi-permeable selective barrier that allows the controlled passage of fluids, molecules and cells to and from the bloodstream. This function relies on the organization of cell-cell junctions, orchestrated notably through VE-cadherin-based adherens junctions (AJs [1,2]. Angiogenic and inflammatory factors elevate endothelial permeability and operate through various signaling pathways; this can involve both transcriptional control of VE-cadherin and post-translational modifications of AJ-enriched proteins, such as phosphorylation of VE-cadherin and its partners, VE-cadherin internalization and cytoskeleton contractility [1,3-8]. Of note, VE-cadherin expression and trafficking control AJ organization, as well as composition of tight junctions (TJs and *vice versa* [9,10]. Indeed, claudin-5-dependent TJs are not functional in VE-cadherin (*CDH5*-null endothelial cells [9,11]. From a molecular standpoint, VE-cadherin sustains the activation of the PI-3 kinase (PI3K/AKT pathway, and the subsequent phosphorylation of the forkhead repressor transcription factor FoxO1, leading to its inhibition [9,11]. Conversely, in cells lacking VE-cadherin, non-phosphorylated active FoxO1 accumulated within the nucleus where *CLDN5* gene expression is constitutively silenced. Consequently, this effect was lost upon rescue of VE-cadherin expression. Modulation of the FoxO1 pathway might thus coordinate the composition of AJs and TJs in endothelial cells, while involved in vascular homeostasis and endothelial proliferation [9,11-13].

Besides phosphorylation, ubiquitylation can also take part in trafficking and degradation of adhesion molecules, as envisioned by early reports on cadherin internalization [14,15]. Proteasome-mediated degradation was indeed proposed to coordinate VE-cadherin stability and therefore AJ architecture and endothelial barrier

integrity [4,15]. For instance, internalized VE-cadherin could be processed through a lysosomal/proteasome pathway [15-17]. More recently, inflammatory agents, such as bradykinin and histamine, were established to provoke VE-cadherin ubiquitylation *in vitro* and *in vivo* [4]. This process was suggested to be required for VE-cadherin internalization and vascular barrier opening. Interestingly, blood-brain barrier damage was shown to be associated with occludin ubiquitylation and degradation [18]. Furthermore, the viral transmembrane ubiquitin ligase K5 encoded by the Kaposi Sarcoma Herpes Virus, which displays some homologies with the MARCH E3 ubiquitin ligase family, was shown to down-regulate membrane availability of host targets such as CD31/PECAM, VE-cadherin and α, β, γ-catenins, and therefore impacts on endothelial l-cell remodeling and barrier function [19,20].

Although lysosomal trafficking and ubiquitylation of endothelial junctional proteins appear intertwined, the ubiquitin ligases involved in theses processes are yet to be characterized. Here, we inferred that endosome/lysosome resident E3 ubiquitin ligases might contribute to endothelial barrier permeability. Therefore, we deployed a siRNA library screen that targets transmembrane E3 ubiquitin ligases and identified MARCH3 as a regulator of endothelial permeability in response to inflammatory factors.

Results

siRNA library screen identifies the E3 ubiquitin ligase MARCH3 in the endothelial barrier function.

To identify transmembrane E3 ubiquitin ligases potentially interfering with cytokine-induced permeability, human umbilical vein endothelial cells (HUVECs were transfected with siRNA duplexes against 46 E3 ubiquitin ligases (2 sequences/target, [21] or with non-silencing RNA (sic, 4 sequences [21]. Cells were seeded on semi-porous collagen-coated membranes for permeability assays [3,22]. When knocked down, none of the tested E3 ubiquitin ligases further exacerbated IL-8- and histamine-promoted permeability (Table S1. Conversely, the silencing of nine of them (namely BFAR, MARCH2, MARCH3, MARCH6, RNF122, RNF133, RNF152, RNF175, and TRIM59 was sufficient to quell IL-8-induced permeability (Fig. 1A, left panel, green and yellow dots. Amongst these hits, MARCH3, RNF152 and TRIM59 were shared in the histamine-triggered permeability screen (Table S1, Fig. 1A, right panel, green and yellow dots. Based on the literature, we further focused on MARCH3 (Fig. 1A, green dots), as it

has been previously linked to the endocytosis and trafficking of plasma membrane proteins [23,24]. The silencing of MARCH3 in human endothelial cells led to a significant reduction in both IL-8- and histamine-promoted permeability by around 40%, while sparing non stimulated cells (Fig. 1A-B, Table S1). To further validate MARCH3 as a negative regulator of endothelial integrity, the permeability of human endothelial cell monolayers was next challenged using independent siRNA sequences (Fig. 1C), whose efficiency was evaluated through RT-PCR to around 60% of extinction for the most robust one (Fig. 1C). Of note, the transcript levels of MARCH2, one of the closest homologue of MARCH3 remained unaltered (Fig. 1C). In these conditions, MARCH3 silencing impaired the permeability increases in both macrovascular (HUVECs, [25]) and microvascular (hCMEC/D3, [26,27]) endothelial cells (Fig. 1D-E). Thus, our data identified MARCH3 as a lysosomal component involved in cytokine-provoked endothelial permeability elevation.

MARCH3-silenced endothelial cells exhibited strengthened cell-cell junctions.

Because of the prominent role of cell-cell contacts in orchestrating the endothelial barrier function [3,4,8,9], we next explored whether MARCH3 silencing impacts on endothelial junctional organization. Interestingly, neither cell viability nor cell density was affected by MARCH3 depletion (Fig. 2A-B. Furthermore, confocal analysis of three-days old endothelial monolayers revealed that IL-8 induced an overall reorganization of phalloidin-labeled cell borders (Fig. 2C-D. However, the chemokine failed to do so in MARCH3-depleted endothelial cells (Fig. 2C-D, suggesting again that the reduction of MARCH3 expression levels opposed to IL-8, provoked junctional remodeling and subsequent increases in endothelial permeability. In keeping with this idea, immunofluorescence staining on three-days old monolayers unveiled a discrete but significant increase in VE-cadherin staining intensity at the borders of adjacent cells (Fig. 2E. This was corroborated by an augmentation in surface-exposed VE-cadherin, as evaluated by flow cytometry (Fig. 2F. Thus, our data support the idea that endothelial adherens junctions are strengthened in MARCH3-silenced cells.

Tight junctions are strengthened in MARCH3-depleted cells.

To further explore the mechanisms by which MARCH3 depletion prevents permeability increases, we next conducted a gene array analysis. The transcriptome of non-silencing control RNA-transfected human brain endothelial cells (sic was compared to the one of MARCH3 siRNA-transfected cells. This unbiased transcriptomic analysis identified few

protein encoding RNA (67% of total modified sequences) that were consistently up- (49%) or down-regulated (51%) in MARCH3-depleted cells (Table S2, Fig. 3A-C). Among the up-regulated genes was *OCLN*, which encodes the TJ protein occludin (Table S2, Fig. 3A-C). Indeed, RT-PCR analysis confirmed that the siRNA-mediated down-regulation of *MARCH3* was accompanied with an augmentation of *OCLN* transcription (Fig. 3C-D). Furthermore, *CLDN5* messengers were also elevated, while *CDH5* gene expression was only slightly enhanced (Fig. 3D). In agreement with this, the levels of occludin and claudin-5 TJ proteins were strongly augmented in the absence of MARCH3 (Fig. 3E). Once again, VE-cadherin expression was only mildly affected, suggesting that unlike occludin and claudin-5, the effect of MARCH3 depletion on VE-cadherin expression is likely indirect and might rather reflect a positive feedback loop, ignited through TJ stabilization (Fig. 2E-F) [9]. At the level of junctional organization, this results in reinforced TJ organization, as illustrated by augmented ZO-1 recruitment at cell borders (Fig. 3F). Thus, MARCH3 silencing, which prevents permeability increases, drives the up-regulation of TJ protein expression that may ultimately culminate in the strengthening of endothelial cell-cell junctions.

MARCH3 impact on *OCLN* gene expression relies on the FoxO pathway.

The forkhead transcription repressor factor FoxO1 controls claudin-5 protein expression [9,13], and was more recently found involved in vascular remodeling [12]. Remarkably, MARCH3 depletion in three-days old starved endothelial cell monolayers was sufficient to enhance the phosphorylation of AKT and FoxO1/3, a signature for the inhibition of this transcription factor (Fig. 4A). In line with this, FoxO1 nuclear accumulation was reduced upon MARCH3 silencing, as examined by immunofluorescence-based confocal analysis (Fig. 4B). We next investigated whether the effect of MARCH3 silencing on occludin expression was mediated through FoxO1 activity. To this end, endothelial cells were challenged with the well-characterized FoxO1 inhibitor AS1708727 [28]. Interestingly, we found that FoxO1 inhibitor treatment was sufficient to elevate *OCLN* expression, while leaving intact *MARCH3* mRNA levels (Fig. 4C). Moreover, pharmacological blockade of FoxO1 blunted histamine- and IL-8-induced permeability (Fig. 4D). As FoxO1 inhibition phenocopied MARCH3 depletion, it may act through the inhibition of the transcriptional repression activity of FoxO1, as previously demonstrated in the context of the *CLDN5* promoter [9].

Collectively, our data favor a model in which MARCH3 sustains the basal activation of FoxO1 that counterpoises barrier reinforcement.

Discussion

In conclusion, our data show that the late endosome/lysosome-anchored MARCH3 E3 ligase controls the expression of the TJ proteins, occludin and claudin-5, most likely via its impact on the transcriptional repressor FoxO. Meanwhile, the overall cell-cell junctions appeared reinforced and VE-cadherin expression affected, although to a lesser extent. We thus unmasked MARCH3 as a novel regulator of the endothelial barrier, as its silencing allows endothelial cells to resist to cytokine-triggered cortical actin remodeling and permeability increase. From a molecular standpoint, our results are reminiscent of the signaling pathway operating downstream of AJ and regulating claudin-5 expression, where FoxO plays an instrumental role in steady state and/or recovery of the endothelial barrier integrity [9,13]. Indeed, MARCH3 silencing causes up-regulation of both claudin-5 and occludin expression, which in turn might strengthen TJ architecture.

Further studies are required to identify MARCH3 molecular targets, as well as the type of ubiquitin modifications involved. Nevertheless, our study highlights the potential importance of ubiquitin ligases, particularly deubiquitylating enzymes, in modulating the composition of the endothelial junctions. Of note, it has been recently reported that occludin can be regulated by ubiquitin-targeted degradation [18,29] during the course of permeability increase. Interestingly, at least two different lysine residues on claudin have been reported to serve as ubiquitin chain acceptors [30,31]. This raised the possibility that MARCH3 might directly or indirectly modulate the ubiquitination/degradation status of tight junction protein complexes and requires further investigation.

In addition, the E3 ubiquitin ligase RNF152, which was found in our initial screen (Table S1), was recently acknowledged to direct the ubiquitylation of the RagA GTPase in response to amino acid starvation and thus to modulate mTORC1 lysosomal signaling [32]. Although we did not pursue on RNF152 in our study, it may be interesting to investigate the possible synergy between RNF152 and MARCH3 in regards to mTORC1 and lysosomal signaling in endothelial homeostasis and barrier integrity. There is now growing evidence that mTORC1 contributes to endothelial homeostasis [33], while

FoxO1 emerged as an instrumental mediator of vascular remodeling operating at the interface between metabolic activity and quiescence/proliferation balance [12].

In conclusion, MARCH3 might sustain the basal activation of FoxO1, which can then be modulated to ensure a rapid and adaptive response of the endothelium. A better knowledge on the basic mechanisms involved in integrating microenvironmental cues and fundamental signaling pathways might improve our understanding of vascular dysfunctions, including exacerbated permeability that occurs in many diseases and man pathologies.

Materials and Methods

Cell culture and transfections

Human umbilical vein endothelial cells (Eahy926 HUVECs) were purchased from ATCC and maintained in DMEM plus 10% fetal bovine serum (Life Technologies). Human cerebral microvascular endothelial cells (hCMEC/D3, [27]) were grown on collagen-coated plates in EBM2 complete medium (Lonza). Cells were transfected using ofectamine RNAimax (Life Technologies) according to the manufacturer's instructions. Non-silencing (Med GC) and MARCH3-targetting Stealth siRNA were from Life Technologies (#1 5'-UGGAGGAUUGUGGCAGCCUAGUGAA, #2 5'-CGGGCAGCUGCUGUCAACAGUAGUG, #3 5'-AGGCCGUUAGUGGAGUGGCUGAGAA). The E3 ubiquitin ligase-targeting siRNA Mission library was designed with Sigma [21].

Permeability assays

Permeability assays were performed as described previously in [25,27]. Briefly, 10^5 transfected HUVECs and 5.10^5 hCMEC/D3 cells were seeded onto collagen-coated 3.0 and 0.4 µm pore size PTFE membrane inserts (Corning), respectively. The passage of FITC-labeled 40kDa dextran (Life Technologies) was measured 30 min after IL-8 (50 ng/ml) or histamine (100 mM) challenge using a BMG Labtech automate plate reader. Screening on IL-8 and histamine-treated cells was conducted as described previously [27]. The library consists of 4 non-silencing sequences (sic) and 2 sequences per target [21]. Non-treated cells were included for the 4 sic-transfected conditions only, to serve as internal controls for histamine and IL-8 action.

Reagents and Antibodies

FoxO1 inhibitor AS1708727 was from Merck and used at 100 nM. Primary antibodies used were: VE-cadherin, GAPDH, and tubulin (Santa Cruz), occludin and claudin-5 (Life Technologies), p-FoxO1, p-FoxO1/3, p-AKT, and AKT (Cell Signaling). Primary antibodies were diluted at 1/1000 for western-blots. HRP-coupled antibodies were from Jackson Immunoresearch (1/5000 dilution).

Immunofluorescence

Samples for immunofluorescence were processed as described in [34]. Briefly, samples were fixed in paraformaldhedyde 4%, permeabilized in Triton 0.5% and blocked in PBS-BSA 3%. Primary antibodies were goat anti-VE-cadherin (1/200 dilution, Santa Cruz), rabbit anti-FoxO1/3 (1/100 dilution, Cell Signaling) and mouse anti-ZO1 (1/200 dilution, BD transduction laboratories). Secondary antibodies were from Life Technologies (AlexaFluor488 conjugated, 1/500 dilution). Actin cytoskeleton was stained using Alexa488-conjugated phalloidin (1/1000 dilution, Life Technologies). Samples were processed in parallel, mounted in DAPI-containing fluoromount (Life Technologies) and imaged using similar settings on confocal microscope (Nikon A1 Rsi, Micropicell, Nantes, France). Images were prepared with Image J software and blinded post-analysis performed by two independent individuals.

Flow Cytometry

Cells were gently scratched and processed for flow cytometry as described in [34]. Briefly, cells were incubated at 4°C with IgG2a PE-conjugated anti-VE-cadherin antibodies and control immunoglobulins (R&D). 10.000 events were gated on an Accuri C6 cytometer (BD Biosciences) and analyzed using FlowJo.

Western-Blots and RT-PCR

Total cell lysates were prepared and processed for western-blots as described in [34]. Membranes were imaged using the Fusion FX7 chemiluminescence system (Vilber). RT-PCR were conducted as described in [34].

Transcriptome analysis

The expression profile of human brain endothelial cells, either control or MARCH3-depleted (two days post-transfection) was performed with the HG-U133 Plus 2.0 Affymetrix GeneChip arrays (Genomic' Platform, Institute Cochin, Paris, France). Supervised clustering analysis of these microarrays was then conducted using p value >

0.05 and fold change + 1.2. A final list of 513 genes was found down- or up-regulated (Table S2).

knowledgments

The authors are thankful to the present and past members of SOAP laboratory in Institut Cochin, Paris, France and CRCNA, Nantes, France, especially to Elizabeth Harford-Wright and Jagoda Hebda. We thank Sebastien Jacques and Florent Dumont (Genom'IC Platform, Institut Cochin, Paris, France) for their help with the gene array analysis.

Author contributions

HML designed the research, conducted the experiments, and analyzed the data; GAG conducted the experiments and analyzed the data; LT designed the research, conducted the experiments, and analyzed the data; SA conducted the experiments and analyzed the data; NB designed the research, conducted the experiments, and analyzed the data; JG designed the research, conducted the experiments, analyzed the data, and wrote the manuscript. All authors have read and approved the manuscript.

Funding

This research was funded by: Fondation pour la Recherche Médicale, Institut National du Cancer, Fondation ARC pour la recherche contre le Cancer, Ligue Nationale contre le Cancer comité Pays-de-la-Loire, comité Maine et Loire, and comité Sarthe, and Connect Talent grant from Region Pays-de-la-Loire and Nantes Metropole.

References

[1] Gavard, J. (2009). Breaking the VE-cadherin bonds. FEBS Lett 583, 1-6.

[2] Dejana, E., Tournier-Lasserve, E. and Weinstein, B.M. (2009). The control of vascular integrity by endothelial cell junctions: molecular basis and pathological implications. Dev Cell 16, 209-21.

[3] Gavard, J. and Gutkind, J.S. (2006). VEGF controls endothelial-cell permeability by promoting the beta-arrestin-dependent endocytosis of VE-cadherin. Nat Cell Biol 8, 1223-34.

[4] Orsenigo, F. et al. (2012). Phosphorylation of VE-cadherin is modulated by haemodynamic forces and contributes to the regulation of vascular permeability in vivo. Nat Commun 3, 1208.

[5] Gaengel, K. et al. (2012). The sphingosine-1-phosphate receptor S1PR1 restricts sprouting angiogenesis by regulating the interplay between VE-cadherin and VEGFR2. Dev Cell 23, 587-99.

[6] Conway, D.E., Breckenridge, M.T., Hinde, E., Gratton, E., Chen, C.S. and Schwartz, M.A. (2013). Fluid shear stress on endothelial cells modulates mechanical tension across VE-cadherin and PECAM-1. Curr Biol 23, 1024-30.

[7] Stockton, R.A., Schaefer, E. and Schwartz, M.A. (2004). p21-activated kinase regulates endothelial permeability through modulation of contractility. J Biol Chem 279, 46621-30.

[8] Bentley, K. et al. (2014). The role of differential VE-cadherin dynamics in cell rearrangement during angiogenesis. Nat Cell Biol 16, 309-21.

[9] Taddei, A. et al. (2008). Endothelial adherens junctions control tight junctions by VE-cadherin-mediated upregulation of claudin-5. Nat Cell Biol 10, 923-34.

[10] Gavard, J. and Gutkind, J.S. (2008). VE-cadherin and claudin-5: it takes two to tango. Nat Cell Biol 10, 883-5.

[11] Oellerich, M.F. and Potente, M. (2012). FOXOs and sirtuins in vascular growth, maintenance, and aging. Circ Res 110, 1238-51.

[12] Wilhelm, K. et al. (2016). FOXO1 couples metabolic activity and growth state in the vascular endothelium. Nature 529, 216-20.

[13] Gao, F. et al. (2016). Akt1 promotes stimuli-induced endothelial-barrier protection through FoxO-mediated tight-junction protein turnover. Cell Mol Life Sci

[14] Fujita, Y., Krause, G., Scheffner, M., Zechner, D., Leddy, H.E., Behrens, J., Sommer, T. and Birchmeier, W. (2002). Hakai, a c-Cbl-like protein, ubiquitinates and induces endocytosis of the E-cadherin complex. Nat Cell Biol 4, 222-31.

[15] Xiao, K., Allison, D.F., Kottke, M.D., Summers, S., Sorescu, G.P., Faundez, V. and Kowalczyk, A.P. (2003). Mechanisms of VE-cadherin processing and degradation in microvascular endothelial cells. J Biol Chem 278, 19199-208.

[16] Nanes, B.A., Chiasson-MacKenzie, C., Lowery, A.M., Ishiyama, N., Faundez, V., Ikura, M., Vincent, P.A. and Kowalczyk, A.P. (2012). p120-catenin binding masks an endocytic signal conserved in classical cadherins. J Cell Biol 199, 365-80.

[17] Xiao, K., Allison, D.F., Buckley, K.M., Kottke, M.D., Vincent, P.A., Faundez, V. and Kowalczyk, A.P. (2003). Cellular levels of p120 catenin function as a set point for cadherin expression levels in microvascular endothelial cells. J Cell Biol 163, 535-45.

[18] Zhang, G.S. et al. (2013). The gamma-secretase blocker DAPT reduces the permeability of the blood-brain barrier by decreasing the ubiquitination and

degradation of occludin during permanent brain ischemia. CNS Neurosci Ther 19, 53-60.
[19] Mansouri, M., Rose, P.P., Moses, A.V. and Fruh, K. (2008). Remodeling of endothelial adherens junctions by Kaposi's sarcoma-associated herpesvirus. J Virol 82, 9615-28.
[20] Mansouri, M., Douglas, J., Rose, P.P., Gouveia, K., Thomas, G., Means, R.E., Moses, A.V. and Fruh, K. (2006). Kaposi sarcoma herpesvirus K5 removes CD31/PECAM from endothelial cells. Blood 108, 1932-40.
[21] Hatchi, E.M., Poalas, K., Cordeiro, N., N'Debi, M., Gavard, J. and Bidere, N. (2014). Participation of the E3-ligase TRIM13 in NF-kappaB p65 activation and NFAT-dependent activation of c-Rel upon T-cell receptor engagement. Int J Biochem Cell Biol 54, 217-22.
[22] Dwyer, J. et al. (2015). The G-protein exchange factor SWAP70 mediates vGPCR-induced endothelial plasticity. Cell Commun Signal 13, 11.
[23] Fukuda, H., Nakamura, N. and Hirose, S. (2006). MARCH-III Is a novel component of endosomes with properties similar to those of MARCH-II. J Biochem 139, 137-45.
[24] Fatehchand, K. et al. (2015). Toll-like receptor 4 ligands down-regulate FcgammaRIIb via MARCH3-mediated ubiquitination. J Biol Chem
[25] Gavard, J., Hou, X., Qu, Y., Masedunskas, A., Martin, D., Weigert, R., Li, X. and Gutkind, J.S. (2009). A role for a CXCR2/phosphatidylinositol 3-kinase gamma signaling axis in acute and chronic vascular permeability. Mol Cell Biol 29, 2469-80.
[26] Weksler, B.B. et al. (2005). Blood-brain barrier-specific properties of a human adult brain endothelial cell line. FASEB J. 19, 1872-4.
[27] Le Guelte, A. et al. (2012). Semaphorin 3A elevates endothelial cell permeability through PP2A inactivation. J Cell Sci 125, 4137-46.
[28] Sunayama, J. et al. (2010). Dual blocking of mTor and PI3K elicits a prodifferentiation effect on glioblastoma stem-like cells. Neuro Oncol 12, 1205-19.
[29] Murakami, T., Felinski, E.A. and Antonetti, D.A. (2009). Occludin phosphorylation and ubiquitination regulate tight junction trafficking and vascular endothelial growth factor-induced permeability. J Biol Chem 284, 21036-46.
[30] Mandel, I., Paperna, T., Volkowich, A., Merhav, M., Glass-Marmor, L. and Miller, A. (2012). The ubiquitin-proteasome pathway regulates claudin 5 degradation. J Cell Biochem 113, 2415-23.
[31] Takahashi, S., Iwamoto, N., Sasaki, H., Ohashi, M., Oda, Y., Tsukita, S. and Furuse, M. (2009). The E3 ubiquitin ligase LNX1p80 promotes the removal of claudins from tight junctions in MDCK cells. J Cell Sci 122, 985-94.
[32] Deng, L. et al. (2015). The ubiquitination of rag A GTPase by RNF152 negatively regulates mTORC1 activation. Mol Cell 58, 804-18.
[33] Sun, S. et al. (2015). Constitutive Activation of mTORC1 in Endothelial Cells Leads to the Development and Progression of Lymphangiosarcoma through VEGF Autocrine Signaling. Cancer Cell 28, 758-772.
[34] Leclair, H.M., Dubois, S.M., Azzi, S., Dwyer, J., Bidere, N. and Gavard, J. (2014). Control of CXCR2 activity through its ubiquitination on K327 residue. BMC Cell Biol 15, 38.

Figure Legends

Figure 1. A siRNA library screen identifies the E3 ubiquitin ligase MARCH3 in the endothelial barrier function.

(**A**) HUVECs were transfected with two siRNA sequences targeting 46 transmembrane-anchored E3 ubiquitin ligases (Table S1, [21]) or non-silencing control duplexes RNA (sic) and plated onto collagen-coated inserts. Three days later, monolayers were starved overnight prior 30 min stimulation with either IL-8 (50 ng/ml) or histamine (100 mM). Sic-transfected untreated and treated cells were used as internal controls. FITC-dextran permeability was expressed as percentage of inhibition with respect to sic-transfected treated cells (% of siRNA control). Hits were considered, when permeability was reduced by a third (yellow dots). MARCH3 is shown in green. (**B**) HUVECs were transfected with either non-silencing duplexes (sic) or MARCH3-targeting siRNA (siM3, from the library panel A). Permeability was assessed upon IL-8 and histamine challenge three days later. (**C**) HUVECs were transfected with three different siRNA sequences targeting MARCH3 (siM3). Knockdown efficiency was assessed by RT-PCR and quantitative densitometry represented as percentage of inhibition (% inh.).. Scans are representative of two independent experiments. (**D-E**) FITC-dextran permeability was measured in similarly treated sic- and siM3-transfected HUVECs (D) and brain endothelial cells hCMEC/D3 (E). Values were expressed as a fold to untreated sic-transfected cells (ctl). Red/blue columns were compared to the black ones. In addition, $p<0.001$ and $p<0.01$ for black columns compared to the white ones in (D) and (E), respectively. All panels are representative of at least three independent experiments, except when specified. ANOVA test and T-test *, $p<0.05$; **, $p<0.01$.

Figure 2. MARCH3-silenced endothelial cells exhibited strengthened cell-cell junctions.

(**A-F**) HUVECs were transfected with siM3 or sic and harvested three days later. (**A**) Viability was measured by MTT in complete medium. Graph shows the mean optical densities (OD, as indicated). (**B**) Cell density was assessed by the ratio between cell-covered area/total culture areas by Image J software (Fiji). (**C**) The organization of cell-cell contact was estimated with phalloidin staining at cell borders. Cells engaged with at least 4 neighboring cells and exhibiting at least two ‘zigzag’ patterns at cell-cell contacts

were counted as positive. (**D**) Confocal analysis of cortical actin organization through phalloidin staining in cells that were left untreated (control) or challenged with IL-8 (30 min, 50 ng/ml). Higher magnifications are shown to depict cell-cell contacts. Scale bars: 10 µm. (**E-F**) Confocal analysis (E) and flow cytometry analysis (F) of cell surface VE-cadherin (VE-cad) in sic- or siM3-transfected cells. Scale bars: 10 µm. Graph shows ratio of pixel intensities between sic/siM3 conditions from 5 random pictures in 3 independent experiments. All panels are representative of at least three independent experiments, except when specified. T-test *, $p<0.05$; **, $p<0.01$.

Figure 3. Tight junctions are strengthened in MARCH3-depleted cells.

(**A**) Gene array analysis of siM3-transfected human brain endothelial cells compared to sic-transfected cells (Table S2). Heat-map of up- (>1.25, red) and down-regulated (<1.25, blue) genes, from siM3/sic fold changes in three independent experiments. The repartition of significantly ($p<0.05$) up- and down-regulated sequences is shown (top diagram). Protein coding RNAs (in yellow, 67% of total gene) were then classified according to their fold change of expression (siM3/sic, bottom diagram). (**B-C**) Table includes two of the best down- (blue) and up-regulated (red) genes (symbol names), together with p-value and fold change. Samples used for gene array were further processed for RT-PCR to validate main hits. (**D-E**) mRNA (D) and protein (E) expression of indicated targets were monitored three days post-transfection by RT-PCR and western-blots, respectively. Graphs showed quantification of fold change in three independents experiments. (**F**) Confocal analysis of tight junction-associated protein ZO-1 in sic- or siM3-transfected endothelial cells. Zoom on cell borders is shown on the right panel, together with an inverted image as processed by Image J (Fiji). Scale bars: 10 µm. All panels are representative of at least three independent experiments. T-test *, $p<0.05$; **, $p<0.01$; ***, $p<0.001$.

ure 4. MARCH3 impact on *OCLN* gene expression relies on FoxO.

(**A-B**) Human brain endothelial cells were transfected with siM3 or sic duplexes, processed for western-blots three days later, as indicated. (B) Alternatively, cells were stained for FoxO1 (green) and analyzed by confocal microscopy. Nuclei were counterstained with DAPI (blue). Graph showed the percentage of FoxO1-positive nuclei. Scale bars: 10 µm. n>200 cells, T-test: *, $p<0.05$. (**C**) Cells were exposed to the

FoxO1 inhibitor (AS1708727, iFoxo, 100 nM, three days) or vehicle (dmso) and processed for RT-PCR. (**D**) Permeability assays were performed in non-stimulated (ctl), histamine- (Hista) or IL-8-challenged HUVECs pre-treated with dmso and iFoxo. All panels are representative of at least three independents experiments. ANOVA test *, $p<0.05$; ***, $p<0.001$.

1- A siRNA library screen identifies the E3 ubiquitin ligase MARCH3 in the endothelial barrier function

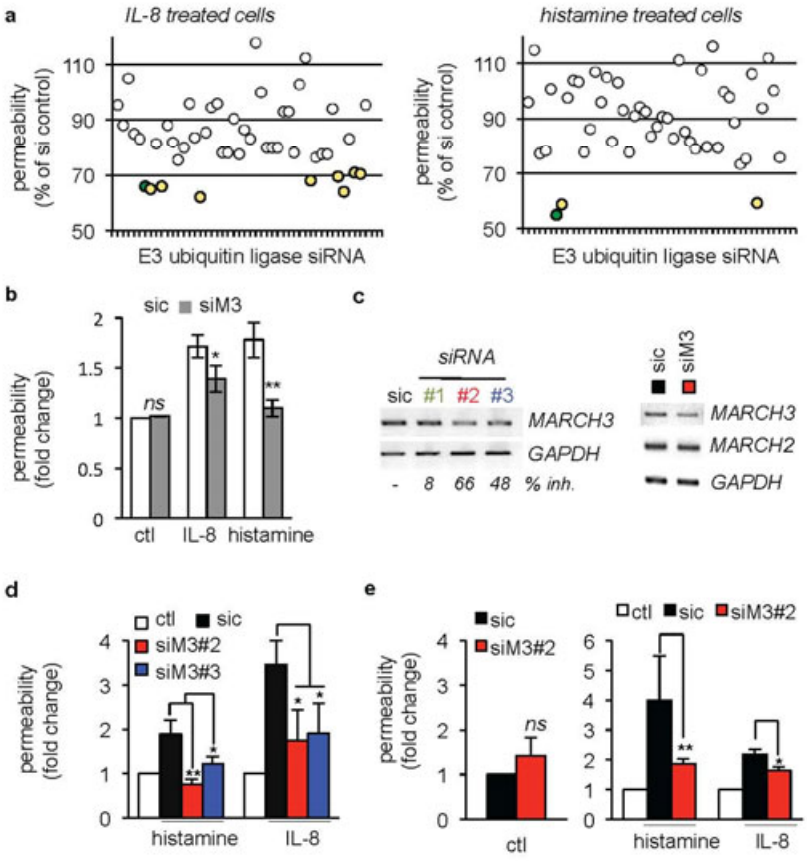

2- MARCH3-silenced endothelial cells exhibited strengthened cell-cell junctions

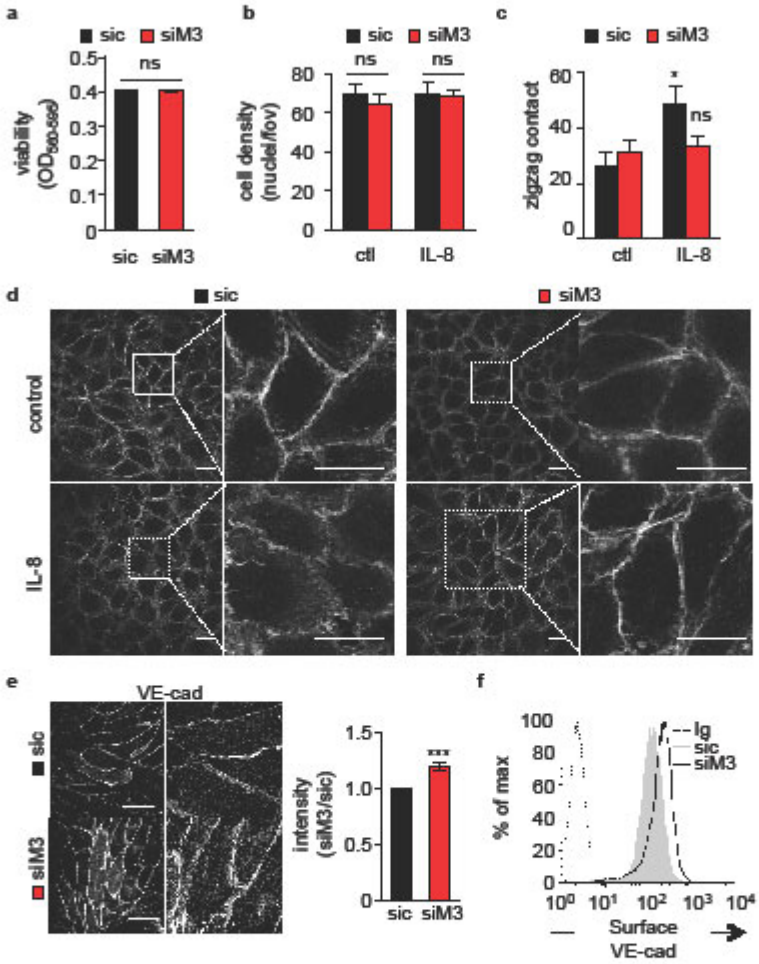

3- Tight junctions are strengthened in MARCH3-depleted cells

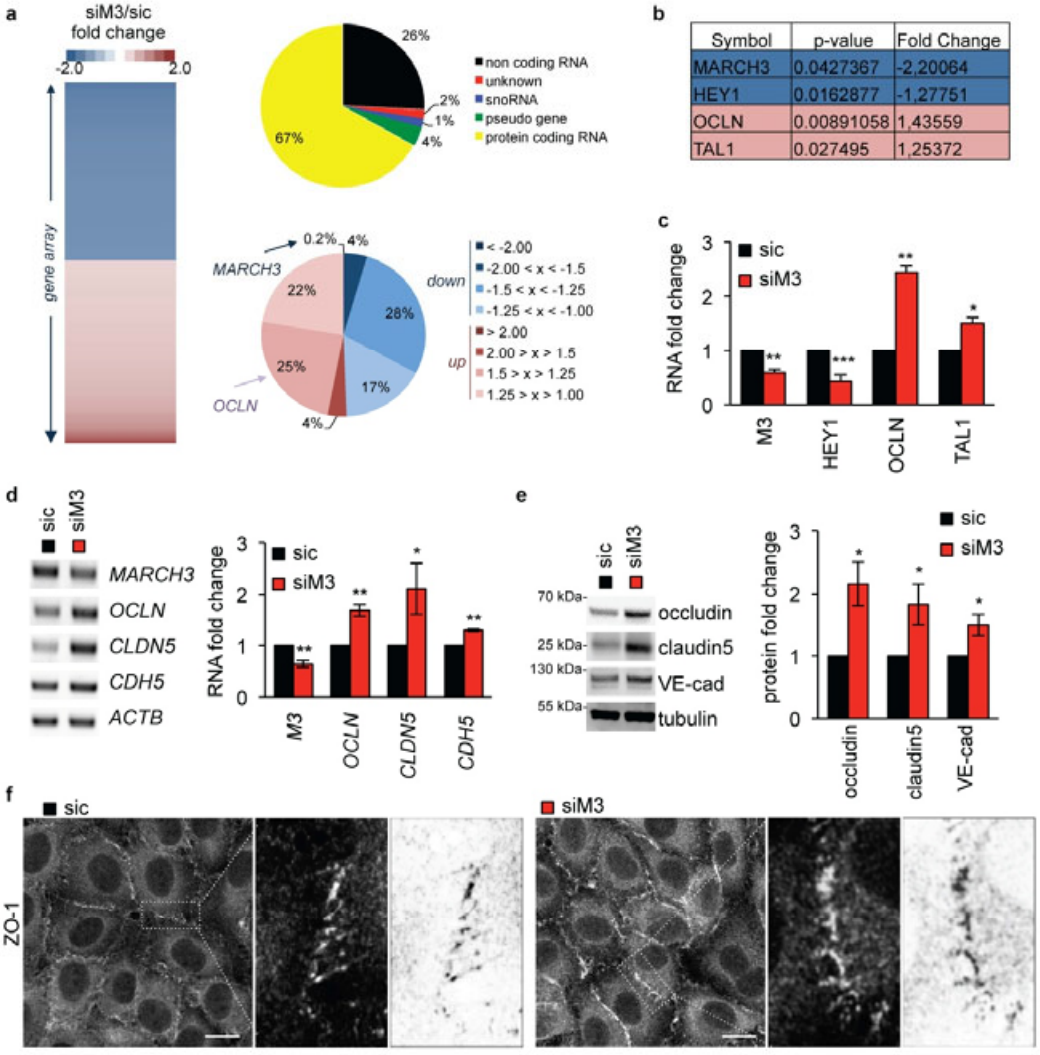

Symbol	p-value	Fold Change
MARCH3	0.0427367	-2,20064
HEY1	0.0162877	-1,27751
OCLN	0.00891058	1,43559
TAL1	0.027495	1,25372

4- MARCH3 impact on *OCLN* gene expression relies on FoxO